

Unresponsiveness to Glibenclamide During Chronic Treatment Induced by Reduction of ATP-Sensitive K⁺ Channel Activity

Jun Kawaki, Kazuaki Nagashima, Jun Tanaka, Takashi Miki, Masaru Miyazaki, Tohru Gono, Noboru Mitsuhashi, Nobuyuki Nakajima, Toshihiko Iwanaga, Hideki Yano, and Susumu Seino

The insulin response to the sulfonylurea glibenclamide was markedly impaired in pancreatic β -cell line MIN6 cells with chronic glibenclamide treatment (MIN6-Glib). The intracellular calcium concentration increased only slightly in response to glibenclamide in MIN6-Glib. While the properties of the voltage-dependent calcium channels were not altered, the conductance of the K_{ATP} channels, the primary target of glibenclamide, was significantly reduced in MIN6-Glib. The ATP-sensitive K⁺ (K_{ATP}) channels in MIN6 cells comprise inwardly rectifying K⁺ channel member Kir6.2 subunits and sulfonylurea receptor (SUR) 1 subunits. MIN6 cells have both high- and low-affinity binding sites for glibenclamide. The binding affinities at these two sites were unchanged, but the maximum binding capacities at both sites were similarly increased by chronic glibenclamide treatment. Both SUR1 and Kir6.2 mRNA levels were not altered, but SUR1 protein was rather increased in MIN6-Glib. In addition, electron microscopic examination revealed a majority of the SUR1 to be present in a cluster near the plasma membrane in control MIN6, while it tends to be distributed in the cytoplasm in MIN6-Glib. These data suggest that chronic glibenclamide treatment causes the defect in acute glibenclamide-induced insulin secretion by reducing the number of functional K_{ATP} channels on the plasma membrane of the β -cells. *Diabetes* 48:2001–2006, 1999

Sulfonylureas such as tolbutamide and glibenclamide are widely used as oral hypoglycemic drugs in the treatment of type 2 diabetes (1). Sulfonylureas are known to increase insulin secretion by directly closing the ATP-sensitive K⁺ (K_{ATP}) channels in

pancreatic β -cells (2–4) which are normally closed by high glucose, causing membrane depolarization and opening of the voltage-dependent Ca²⁺ channels (VDCCs), which allows Ca²⁺ influx and the resultant rise in intracellular Ca²⁺ concentration ([Ca²⁺]_i) that triggers insulin secretion (5–7). We have shown recently that there is no insulin secretory response to either glucose or tolbutamide stimulation in K_{ATP} channel-deficient mice (8). Thus, the K_{ATP} channels in pancreatic β -cells play a critical role in the regulation of both sulfonylurea-induced and glucose-induced insulin secretion.

It has been shown that classical K_{ATP} channels comprise Kir6.2 subunits of the inwardly rectifying K⁺ channel Kir6.0 subfamily (9–11) and sulfonylurea receptor (SUR1 or SUR2) subunits of the ATP binding cassette (ABC) protein superfamily (12–14). The pancreatic β -cell K_{ATP} channel functions as a heterooctameric protein of four Kir6.2 subunits and four SUR1 subunits (15–17). It is thought that while the Kir6.2 subunits form a K⁺ ion-permeable pore and primarily confer ATP inhibition, the SUR1 subunits confer sulfonylurea, diazoxide, and MgADP sensitivities and enhance the sensitivity of Kir6.2 to ATP (18–20).

Although sulfonylureas are known to acutely stimulate insulin secretion, several studies in vivo and in vitro have shown that chronic sulfonylurea treatment can cause impaired sulfonylurea-induced insulin secretion. For example, Karam et al. (21) have reported that exposure of pancreatic β -cells to sustained stimulation by therapeutic doses of sulfonylureas can selectively abolish their responsiveness to acute stimulation with tolbutamide in type 2 diabetes. In addition, prolonged exposure of isolated pancreatic islets to sulfonylurea generates unresponsiveness to the stimulus (22–24). These studies suggest that after chronic exposure to sulfonylurea, the pancreatic β -cells become desensitized to the stimulus. Rabuazzo et al. (24) found that the defect in glibenclamide-induced insulin secretion that occurs after chronic exposure of pancreatic islets to glibenclamide is accompanied by impaired suppression of ⁸⁶Rb⁺ efflux, suggesting that the primary defect in pancreatic β -cells exposed to glibenclamide may be in the K_{ATP} channels. However, how the K_{ATP} channels in pancreatic β -cells might be affected by chronic sulfonylurea treatment is not known.

The present study was designed to investigate the mechanism of the defect in acute sulfonylurea-induced insulin secretion in pancreatic β -cells that are exposed chronically to the same stimuli. Our data suggest that chronic treatment of pancreatic β -cells with sulfonylureas might impair acute sulfonylurea-induced insulin secretion not by desensitizing

From the Departments of Molecular Medicine (J.K., K.N., T.M., N.M., H.Y., S.S.) and Surgical Organ-Pathophysiology (M.M., N.N.), Chiba University Graduate School of Medicine; the Research Center for Pathogenic Fungi and Microbial Toxicoses (T.G.), Chiba University, Chiba; and the Laboratory of Anatomy (J.T., T.I.), Hokkaido University Graduate School of Veterinary Medicine, Sapporo, Japan.

Please address correspondence and reprint requests to Susumu Seino, MD, DMSc, Department of Molecular Medicine, Chiba University Graduate School of Medicine 1–8–1, Inohana, Chuo-ku, Chiba 260–8670, Japan. E-mail: seino@molmed.m.chiba-u.ac.jp.

Received for publication 9 February 1999 and accepted in revised form 11 June 1999.

[Ca²⁺]_i, intracellular calcium concentration; DMEM, Dulbecco's modified Eagle's medium; K_{ATP}, ATP-sensitive K⁺ channel; MIN6-Glib, pancreatic β -cell line MIN6 cells with chronic glibenclamide treatment; SUR, sulfonylurea receptor; VDCC, voltage-dependent Ca²⁺ channel.

SUR1 but by reducing the number of functional K_{ATP} channels on the plasma membrane.

RESEARCH DESIGN AND METHODS

Cell culture and transfection. MIN6 cells were plated at a density of 6×10^4 cells per 10-cm-diameter dish, and were cultured in Dulbecco's modified Eagle's medium (DMEM) containing 25 mmol/l glucose and 10% fetal bovine serum under a humidified condition of 95% air and 5% CO_2 . Two days after plating, 10 μ mol/l glibenclamide was added to the medium. The cells were cultured with the medium containing glibenclamide for 14 days. The cells were trypsinized and replated for the experiments on insulin secretion, glibenclamide binding, electrophysiology, and the measurement of intracellular calcium concentrations ($[Ca^{2+}]_i$). The cells were also harvested for RNA blot and immunoblot analyses and for measurement of insulin content. For electrophysiological experiments, MIN6 cells were replated at a density of 2×10^5 per 3.5-cm-diameter dish containing coverslips and incubated in DMEM supplemented with 10% fetal bovine serum with 10 μ mol/l glibenclamide (for pancreatic β -cell line MIN6 cells with chronic glibenclamide treatment [MIN6-Glib]) or without glibenclamide (for control MIN6 cells). Before the experiments, cells were perfused in the extracellular solution on the perfusion well of the patch clamp system for at least 30 min. For glibenclamide binding experiments in transfected cells, COS-1 cells were cultured in the conditions described above. COS-1 cells at 70% of confluency were transfected with pCMVSUR1 (5 μ g) (10) alone, pCMVSUR1-Kir6.2 (5 μ g) containing a DNA fragment encoding a fusion peptide consisting of an SUR1 subunit and a Kir6.2 subunit (15), or pCMVKir6.2 (5 μ g) (10) and pCMVSUR1 (5 μ g) with LIPO-FECTAMINE and OPTI-MEM I reagents (Life Technologies, Rockville, MD) as previously described (10).

Measurements of insulin secretion and insulin content. After MIN6 cells were cultured in the medium containing glibenclamide for 14 days, they were replated on a 48-well plate at a density of 5×10^4 /well and were incubated with the same medium for 46–50 h. MIN6 cells were preincubated for 30 min in the incubation buffer (154 mmol/l NaCl, 6.2 mmol/l KCl, 3.3 mmol/l $CaCl_2$, 1.5 mmol/l KH_2PO_4 , 1.6 mmol/l $MgSO_4$, 12.4 mmol/l $NaHCO_3$, and 20.0 mmol/l HEPES, pH 7.4) containing 3 mmol/l glucose and 0.2% bovine serum albumin (25). The cells were then stimulated in 500 μ l of the same buffer containing 25 mmol/l glucose, 100 mmol/l glibenclamide, or 60 mmol/l K^+ and 0.2% bovine serum albumin for 30 min. When the concentration of KCl was increased to 60 mmol/l, that of NaCl was decreased to keep the osmolarity of the buffer unchanged. The insulin released into the medium was measured by radioimmunoassay (Eiken Chemical, Tokyo) with rat insulin as standard (26). For measurement of insulin content, MIN6 cells were homogenized in 500 μ l acid-ethanol (37% HCl to 75% ethanol, 15:1000 vol/vol) and extracted at 4°C overnight. A total of 400 μ l of acidic extracts was dried by vacuum, reconstituted, and measured by radioimmunoassay. Insulin content in MIN6-Glib is expressed as percent of the values (nanograms per 10^5 cells) obtained from control MIN6.

Measurement of intracellular calcium concentrations. MIN6 cells were loaded with 2 μ mol/l fura-2 acetoxymethyl ester (Dojindo, Kumamoto, Japan) for 50 min in the incubation buffer described for insulin assay containing 3 mmol/l glucose, and then were mounted on the stage of the microscope. The perfusion rate was approximately 1.0 ml/min at 37°C. Intracellular calcium concentration $[Ca^{2+}]_i$ was measured by a dual-excitation wavelength method (340/380 nm) as described (8). When the concentration of KCl was increased to 60 mmol/l, that of NaCl was decreased to keep the osmolarity of the medium unchanged. $[Ca^{2+}]_i$ was calibrated in droplets containing solutions of known Ca^{2+} concentration using the calibration kit (Molecular Probes, Eugene, OR). Fluorescence emission at 510 nm was monitored and the ratio calculation was digitized every 10 s by a computerized image processor (Argus-100/CA; Hamamatsu Photonics, Hamamatsu, Japan).

Measurement of membrane potentials. The membrane potentials of the MIN6 cells were measured by the perforated patch-clamp method in the current clamp mode (25). The extracellular solution contained 125 mmol/l NaCl, 5 mmol/l KCl, 1.3 mmol/l KH_2PO_4 , 2 mmol/l $CaCl_2$, 1 mmol/l $MgCl_2$, 10 mmol/l HEPES, and 2.8 mmol/l glucose (pH 7.4). The pipette solution contained 130 mmol/l potassium aspartate, 10 mmol/l KCl, 10 mmol/l EGTA, 10 mmol/l MOPS (pH 7.2), and 100 μ g/ml nystatin.

Electrophysiological analysis of VDCCs. The whole-cell Ba^{2+} currents through the VDCCs were recorded as described (27). Briefly, Ba^{2+} was used as a charged carrier for measurement of VDCC currents. The extracellular solution contained 20 mmol/l $Ba(OH)_2$, 20 mmol/l 4-aminopyridine, 110 mmol/l tetraethylammonium hydroxide, 10 mmol/l tetraethylammonium chloride, 140 mmol/l methanesulfonate, and 10 mmol/l 3-(*N*-morpholino) propanesulfonic acid (pH 7.4). The pipette solution contained 10 mmol/l CsCl, 130 mmol/l cesium aspartate, 10 mmol/l EGTA, 5 mmol/l Mg-ATP, and 10 mmol/l 3-(*N*-morpholino) propanesulfonic acid (pH 7.2). Cells were maintained at a holding potential of -70 mV. For recording VDCC currents, square pulses of 400 ms duration at potentials between -40 and $+60$ mV in steps of 10 mV were applied every 4 s. Recordings

were performed by using the EPC-7 patch clamp system (List Electronic, Darmstadt, Germany).

Electrophysiological analysis of K_{ATP} channels. Single-channel recordings were done in the excised inside-out membrane patch configuration, as described (28). The intracellular solution contained 110 mmol/l potassium aspartate, 30 mmol/l KCl, 2 mmol/l $MgSO_4$, 1 mmol/l EGTA, 0.084 mmol/l $CaCl_2$, and 10 mmol/l MOPS (pH 7.2). The pipette solution contained 140 mmol/l KCl, 2 mmol/l $CaCl_2$, and 5 mmol/l MOPS (pH 7.4). For whole-cell recording, the extracellular solution contained 135 mmol/l NaCl, 5 mmol/l KCl, 5 mmol/l $CaCl_2$, 2 mmol/l $MgSO_4$, 5 mmol/l HEPES, and 3 mmol/l glucose (pH 7.4). The pipette solution contained 107 mmol/l KCl, 11 mmol/l EGTA, 2 mmol/l $MgSO_4$, 1 mmol/l $CaCl_2$, and 11 mmol/l HEPES (pH 7.2, adjusted with KOH). Electrophysiological experiments were carried out at 24–26°C.

Glibenclamide binding experiments. Binding experiments of MIN6 cells with or without chronic glibenclamide treatment and COS-1 cells transfected with SUR1 alone, SUR1-Kir6.2 fusion peptide, or SUR1 and Kir6.2 were performed according to the method of Åmmälä et al. (29). Assays were done in the buffer containing 119 mmol/l NaCl, 4.7 mmol/l KCl, 2.5 mmol/l $CaCl_2$, 1.2 mmol/l KH_2PO_4 , 1.2 mmol/l $MgSO_4$, 5.0 mmol/l $NaHCO_3$, and 20.0 mmol/l HEPES (pH 7.4). For 3H -labeled glibenclamide binding studies, the cells were washed twice with the same buffer and resuspended in the same buffer. The cells were then incubated for 1 h at room temperature with 1–30 mmol/l 3H -labeled glibenclamide (DuPont, Boston, MA) at a density of 2.5 – 5.2×10^5 cells per tube in 0.4 ml of the same buffer in the absence or presence of 100 μ mol/l unlabeled glibenclamide. Bound radioligand was separated from free 3H -labeled glibenclamide by rapid vacuum filtration through Whatman GF/C filters (Whatman International, Maidstone, England, U.K.). The filters were washed three times with 4 ml ice-cold buffer and radioactivity was counted by a gamma counter.

RNA blot analyses of SUR1 and Kir6.2. Total RNA was isolated by guanidinium isothiocyanate-CsCl procedure (30). Five micrograms of RNA preparations were denatured, electrophoresed through formaldehyde/agarose gels, and transferred to Duralon membranes (Stratagene, La Jolla, CA). The membranes were hybridized with human insulin cDNA, SUR1 cDNA, or Kir6.2 cDNA probe prepared by nick translation using [^{32}P]dCTP (10).

Immunoblot analysis of SUR1. Anti-SUR1 antibody was raised in a rabbit immunized with the synthetic peptide, which corresponded to 21 amino acid residues (KPEKLLSQKDSVFASFVRADK) in the C-terminus of rat SUR1, and was purified with MabTrap GII (Amersham Pharmacia Biotech, Uppsala, Sweden).

MIN6 cells with or without glibenclamide treatment were lysed, homogenized, and sonicated in lysis buffer containing 10 mmol/l Tris, 2 mmol/l EDTA, 100 mmol/l NaCl, 20% glycerol (pH 7.4), 1 mg/ml leupeptin, 1 mg/ml antipain, 1 mmol/l pepstatin A, and 0.1 mmol/l phenylmethylsulfonyl fluoride. Aliquots of the whole-cell preparations (10 μ g protein/lane) were electrophoresed through 7% SDS-polyacrylamide gel and electrotransferred at 15 V on polyvinylidene difluoride membranes for 1 h. The filters were blocked for 1 h with 5% nonfat dry milk and 10% donkey serum in phosphate-buffered saline with Tween 20 (PBS-Tween; pH 7.4) consisting of 136.9 mmol/l NaCl, 2.7 mmol/l KCl, 10 mmol/l Na_2HPO_4 , 1.8 mmol/l KH_2PO_4 , and 0.1% Tween 20 at room temperature. After washing with PBS-Tween containing 1% nonfat dry milk, the filters were incubated with anti-SUR1 antibody for 2 h. The primary antibody immunoreactions were then visualized with horseradish peroxidase-conjugated donkey anti-rabbit immunoglobulin using an enhanced chemiluminescence system (ECL; Amersham Pharmacia Biotech).

Electron microscopic analysis. MIN6 cells on culture dishes were fixed in 4% paraformaldehyde in 0.1 mol phosphate buffer (pH 7.4) for 4 h. After treatment with a 10% normal goat serum, the cells were incubated with a rabbit anti-SUR1 antiserum diluted in 1:4,000. They were further incubated with colloidal gold (1.4 nm in diameter)-conjugated goat anti-rabbit IgG (Nanoprobes, New York). Following silver enhancement (HQ Silver; Nanoprobes), the samples were dehydrated through a graded series of ethanol and directly embedded in Epon 812 resin. Ultrathin sections were prepared with an ultramicrotome (Leica Ultracut UCT; Nissei Sangyo, Tokyo), stained with uranyl acetate and examined with a transmission electron microscope (H-7100; Hitachi, Tokyo).

Data presentation and statistical analyses. Data are expressed as means \pm SE. The columns and bars in each figure indicate the mean and SE, respectively. Statistical significance was determined by unpaired *t* test. *P* values of <0.05 were counted significantly different.

RESULTS

Effects of chronic glibenclamide treatment on insulin secretion and insulin content. Basal insulin secretion in the presence of 3 mmol/l glucose (expressed as nanograms per well per 30 min) in MIN6-Glib was significantly higher than that in untreated control MIN6 cells (MIN6-Glib, 5.5 ± 0.4 ng \cdot well $^{-1} \cdot$ 30 min $^{-1}$, $n = 35$; control, 2.8 ± 0.2 ng \cdot well $^{-1} \cdot$

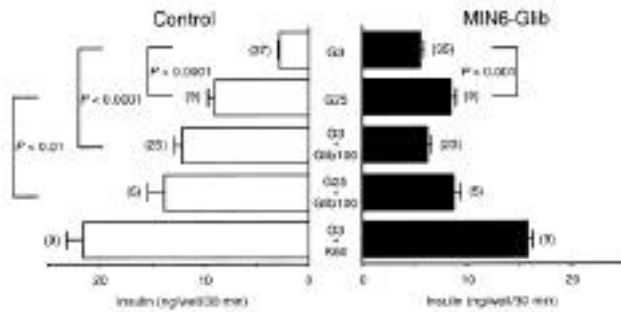


FIG. 1. Insulin secretion. G3, basal insulin secretion in the presence of 3 mmol/l glucose; G25, insulin secretion stimulated by 25 mmol/l glucose; G3 + Glib100, 100 nmol/l glibenclamide in the presence of 3 mmol/l glucose; G25 + Glib100, 100 nmol/l glibenclamide in the presence of 25 mmol/l glucose; G3 + K60, 60 mmol/l K^+ in the presence of 3 mmol/l glucose. Control, untreated MIN6 cells; MIN6-Glib, MIN6 cells treated with glibenclamide for 14 days. Numbers in parentheses indicate the number of experiments.

30 min⁻¹, $n = 37$) ($P < 0.0001$) (Fig. 1). Glibenclamide-induced insulin secretion in the presence of 3 mmol/l glucose in MIN6-Glib was markedly lower than that in control (MIN6-Glib, 6.2 ± 0.5 ng · well⁻¹ · 30 min⁻¹, $n = 23$; control, 12.2 ± 0.7 ng · well⁻¹ · 30 min⁻¹, $n = 25$) ($P < 0.0001$). Insulin response to 100 nmol/l glibenclamide plus 25 mmol/l glucose stimulation in MIN6-Glib was also significantly lower than that in control (MIN6-Glib, 8.8 ± 0.7 ng · well⁻¹ · 30 min⁻¹, $n = 5$; control, 13.9 ± 1.5 ng · well⁻¹ · 30 min⁻¹, $n = 5$) ($P < 0.02$). Tolbutamide-induced insulin secretion in the presence of 3 mmol/l glucose in MIN6-Glib also was markedly lower than that in control (data not shown). With 60 mmol/l K^+ stimulation in the presence of 3 mmol/l glucose, insulin secretion in MIN6-Glib was significantly lower than that in control (MIN6-Glib, 15.8 ± 0.5 ng · well⁻¹ · 30 min⁻¹, $n = 9$; control, 21.6 ± 1.6 ng · well⁻¹ · 30 min⁻¹, $n = 9$) ($P < 0.002$). Insulin content in MIN6-Glib was reduced to $76.9 \pm 4.4\%$ of control ($n = 5$, $P < 0.01$). Northern blot analysis revealed that the insulin mRNA levels were not different in MIN6-Glib and control (data not shown).

Effect of chronic glibenclamide treatment on $[Ca^{2+}]_i$. Basal levels of $[Ca^{2+}]_i$ in MIN6-Glib were 185.1 ± 18.4 nmol/l ($n = 75$), a value significantly higher than that for controls (92.2 ± 7.5 nmol/l, $n = 62$) ($P < 0.0001$) (Fig. 2). In contrast to

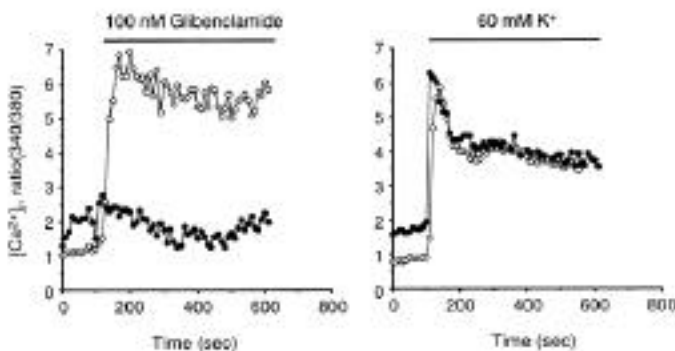


FIG. 2. Intracellular calcium response to 100 nmol/l glibenclamide or 60 mmol/l K^+ . Both stimuli were in the presence of 3 mmol/l glucose. The basal $[Ca^{2+}]_i$ in MIN6-Glib is significantly higher than that in control. Intracellular calcium response to glibenclamide is significantly impaired in MIN6-Glib, compared with control. The degree of the impairment varied among the individual MIN6-Glib cells. Representative examples are shown. ○, control; ●, MIN6-Glib.

controls, however, glibenclamide at 100 nmol/l only slightly increased $[Ca^{2+}]_i$ in MIN6-Glib (Fig. 2).

Effect of chronic glibenclamide treatment on membrane potential. The resting membrane potential in MIN6-Glib was significantly higher than that in controls (MIN6-Glib, -43.3 ± 3.4 mV, $n = 16$; control, -65.4 ± 2.6 mV, $n = 14$) ($P < 0.0001$).

Effects of chronic glibenclamide treatment on VDCCs. Typical L-type VDCC currents were detected in both MIN6-Glib and controls (data not shown). There was no difference in activation and inactivation time courses between MIN6-Glib and controls (data not shown). The current-voltage relationship of the VDCCs in MIN6-Glib was identical to that in controls (Fig. 3).

Effects of chronic glibenclamide treatment on K_{ATP} channels. Single-channel analysis showed unitary conductance, inward rectification (Fig. 4A), and ATP-sensitivity (Fig. 4B) of K_{ATP} channels in MIN6-Glib to be identical to those in control. Glibenclamide at 100 nmol/l inhibited K_{ATP} channel activity in both MIN6-Glib and control (data not shown). Whole-cell recordings showed that in the absence of ATP in the pipette solution, a progressive increase in K^+ conductance in response to ± 10 mV amplitude pulses was detected in control MIN6 cells and that the increased currents were inhibited by addition of glibenclamide (100 nmol/l) (Fig. 4C). In contrast, the K^+ conductance in MIN6-Glib was significantly reduced. ATP-sensitive K^+ conductance, normalized by dividing by membrane capacitance, was significantly reduced in MIN6-Glib (MIN6-Glib, 0.15 ± 0.05 nS/pF, $n = 11$; control, 1.19 ± 0.29 nS/pF, $n = 12$) ($P < 0.02$) (Fig. 4D), indicating impaired K_{ATP} channel conductance in MIN6-Glib.

Effects of chronic glibenclamide treatment on glibenclamide binding properties. Analysis of [³H]glibenclamide binding to MIN6 cells revealed both high-affinity and relatively low-affinity binding sites ("high-affinity" and "low-affinity" sites in this paper). The K_d values of the high- and low-affinity sites in MIN6-Glib were not different from those in control (MIN6-Glib, $K_{d\text{high}} = 2.5 \pm 0.3$ nmol/l, $K_{d\text{low}} = 13.4 \pm 2.3$ nmol/l,

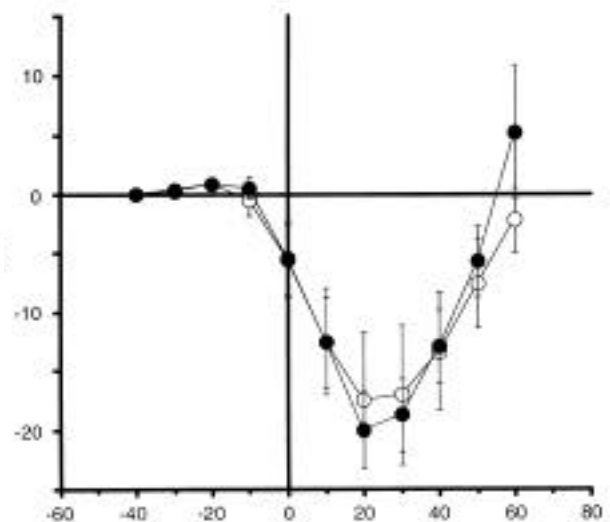


FIG. 3. The current-voltage relationships of VDCCs in MIN6-Glib and control MIN6 cells. Because the membrane area of each cell varied, VDCC currents were normalized by dividing by the membrane capacitance measured for each cell. Values are means \pm SE (MIN6-Glib, $n = 5$; control, $n = 6$). ○, control; ●, MIN6-Glib.

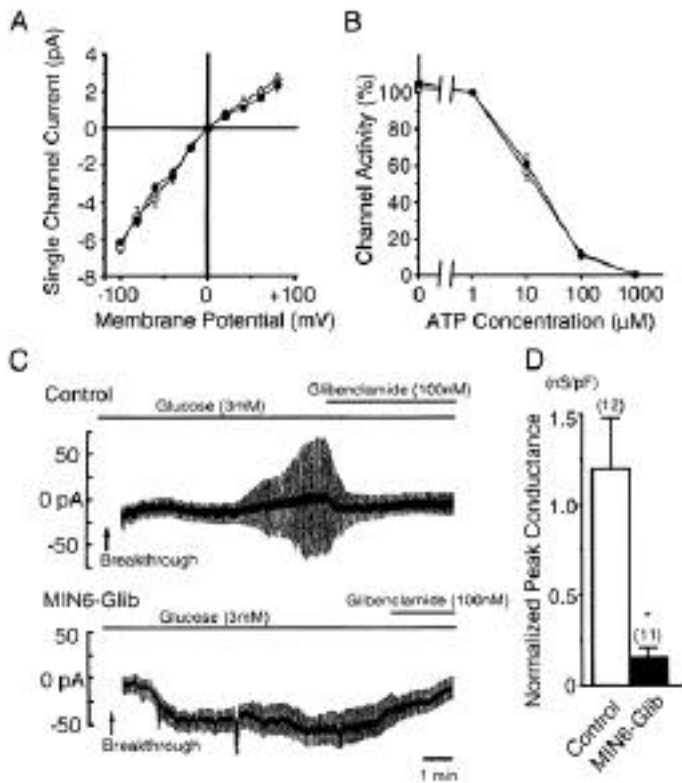


FIG. 4. Electrophysiological analysis of K_{ATP} channels in control and MIN6-Glib. **A:** Current-voltage (I - V) relationships recorded in control (\circ) and MIN6-Glib (\bullet). The number of experiments was three in each case. **B:** Dose-dependent effect of ATP on K_{ATP} channels in control (\circ) and MIN6-Glib (\bullet) ($n = 4-7$). Channel activities are expressed as percent of activity in the presence of $1 \mu\text{mol/l}$ ATP. **C:** Representative traces of whole-cell recordings in control and MIN6-Glib. The holding potential was -70 mV , and alternate voltage pulses of $\pm 10 \text{ mV}$ and 200 ms duration every 2 s were applied. Removal of intracellular ATP beginning at the time indicated (breakthrough) caused a progressive increase in K^+ conductance in response to $\pm 10 \text{ mV}$ amplitude pulses, and addition of 100 nmol/l glibenclamide promptly inhibited the conductance. The recordings were performed in the presence of 3 mmol/l glucose in the extracellular solution. **D:** Normalized K_{ATP} channel conductances in control and MIN6-Glib. Because the membrane area of each cell varied, the K^+ conductance was normalized by dividing by the membrane capacitance measured for each cell. Numbers in parentheses indicate the number of experiments. Values are means \pm SE. $*P < 0.02$.

$n = 4$; control, $K_{d\text{high}} = 1.7 \pm 0.2 \text{ nmol/l}$, $K_{d\text{low}} = 11.6 \pm 1.2 \text{ nmol/l}$, $n = 4$). In contrast, the maximum binding capacities of both the high- and low-affinity sites in MIN6-Glib were not reduced, but were rather increased (MIN6-Glib, $B_{\text{max high}} = 279.9 \pm 23.6 \text{ fmol}/10^6 \text{ cells}$, $B_{\text{max low}} = 699.3 \pm 64.2 \text{ fmol}/10^6 \text{ cells}$, $n = 4$; control, $B_{\text{max high}} = 171.4 \pm 6.5 \text{ fmol}/10^6 \text{ cells}$, $B_{\text{max low}} = 430.5 \pm 34.9 \text{ fmol}/10^6 \text{ cells}$, $n = 4$) ($P < 0.02$) (Fig. 5).

We also examined the binding affinities of glibenclamide to COS-1 cells expressing SUR1 alone (COS-1-SUR1), SUR1-Kir6.2 fusion peptide (COS-1-SUR1-Kir6.2), and SUR1 and Kir6.2 (COS-1-SUR1/Kir6.2). COS-1-SUR1 has only the low-affinity site ($K_{d\text{low}} = 15.5 \pm 3.0 \text{ nmol/l}$, $n = 3$), and COS-1-SUR1-Kir6.2 has only the high-affinity site ($K_{d\text{high}} = 5.2 \pm 0.8 \text{ nmol/l}$, $n = 3$). In contrast, COS-1-SUR1/Kir6.2 has both the high-affinity site and the low-affinity site, with K_d values of the high-affinity site ($K_{d\text{high}} = 5.2 \pm 0.3 \text{ nmol/l}$, $n = 3$) and the low-affinity site ($K_{d\text{low}} = 15.6 \pm 2.8 \text{ nmol/l}$, $n = 3$) that are identical to those in COS-1-SUR1-Kir6.2 and COS-1-SUR1, respectively (Table 1).

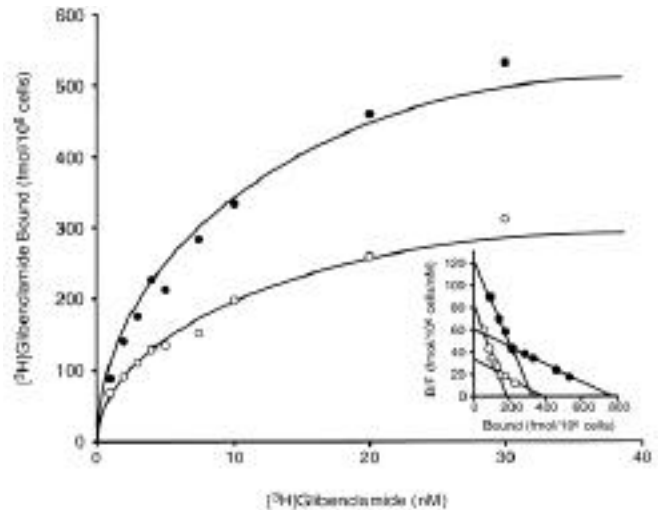


FIG. 5. Analysis of the binding of $[^3\text{H}]$ glibenclamide to MIN6-Glib (\bullet) and control (\circ). **Inset:** Scatchard transformation of the data. The representative plots of 4 experiments are shown.

Effects of chronic glibenclamide treatment on SUR1 and Kir6.2 expression. RNA blot analysis showed no difference in SUR1 and Kir6.2 mRNA levels between MIN6-Glib and control (Fig. 6A). In contrast, immunoblot analysis of whole-cell preparations showed that the SUR1 protein level in MIN6-Glib was higher than that in control (Fig. 6B).

Subcellular localization of SUR1. Immunoreactivity for SUR1 was visualized as an accumulation of gold particles under an electron microscope. In control, the immunoreactivity was localized in restricted regions of the cell surface, showing a patch-like accumulation (Fig. 7A and B). In MIN6-Glib, the immunoreactivity extended to the deeper region of the cytoplasm (Fig. 7C). In some MIN6-Glib, gold particles were distributed diffusely in the cytoplasm (Fig. 7D).

DISCUSSION

We found that chronic glibenclamide treatment of MIN6 cells induces a severe defect in acute glibenclamide-induced insulin secretion, confirming previous studies showing that prolonged exposure of isolated pancreatic islets to sulfonylurea causes unresponsiveness to the same stimulus (22-24). Tolbutamide-induced insulin secretion also was severely impaired in MIN6-Glib (data not shown).

TABLE 1

K_d values of high- and low-affinity binding sites in MIN6 cells with or without chronic glibenclamide treatment and COS-1 cells

	$K_{d\text{high}}$ (nmol/l)	$K_{d\text{low}}$ (nmol/l)
Control MIN6	1.7 ± 0.2	11.6 ± 1.2
MIN6-Glib	2.5 ± 0.3	13.4 ± 2.3
COS-1-SUR1	Absent	15.5 ± 3.0
COS-1-SUR1-Kir6.2	5.2 ± 0.8	Absent
COS-1-SUR1/Kir6.2	5.2 ± 0.3	15.6 ± 2.8

Data are means \pm SE. COS-1-SUR1, COS-1 cells expressing SUR1 alone; COS-1-SUR1-Kir6.2, COS-1 cells expressing the SUR1-Kir6.2 fusion protein; COS-1-SUR1/Kir6.2, COS-1 cells expressing SUR1 and Kir6.2.

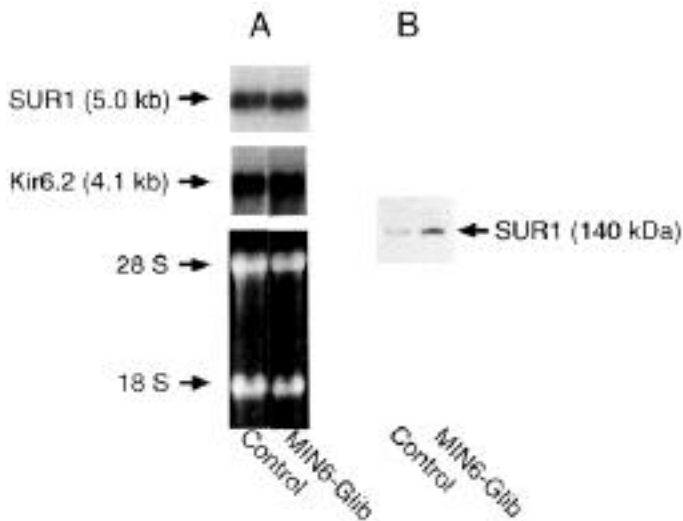


FIG. 6. SUR1 and Kir6.2 expressions. *A*: RNA blot analysis. *Top, middle, and bottom panel* indicate SUR1 transcript, Kir6.2 transcript, and ethidium bromide-stained gel, respectively, before transfer. The sizes of the hybridizing transcripts and 28S and 18S ribosomal RNAs are indicated. *B*: Immunoblot analysis of SUR1. SUR1 protein is detected as 140 kDa.

The insulin response (73.1% of control) to high K^+ stimulation, a most potent stimulus of insulin secretion, was almost parallel to the decrease in insulin content (76.9% of control) in MIN6-Glib. We also found no difference in insulin mRNA levels between MIN6-Glib and control. Because the decrease in insulin content cannot explain the marked reduction in sulfonylurea-induced insulin secretion in MIN6-Glib, these results suggest that the major defect in insulin secretion due to chronic treatment of MIN6 cells with glibenclamide is in steps specific for sulfonylureas.

$[Ca^{2+}]_i$ in pancreatic β -cells is the principal signal for insulin secretion. We have found an elevation of basal $[Ca^{2+}]_i$ and resting membrane potential, which could account for the increase in the basal level of insulin secretion in MIN6-Glib. However, since both the change in $[Ca^{2+}]_i$ in response to high K^+ stimulation and the current-voltage relationship of the VDCCs are not different between MIN6-Glib and control, it is likely that chronic glibenclamide treatment does not directly impair calcium influx through the VDCCs, but that the cause is in the proximal pathway.

Because sulfonylurea-induced insulin secretion depends critically on closure of the K_{ATP} channels in pancreatic β -cells (2–4), chronic glibenclamide treatment could well affect their functional properties and expression. In inside-out patches, the unitary conductance and ATP sensitivity of the K_{ATP} channels in MIN6-Glib were identical to those of control. Glibenclamide at 100 nmol/l, the concentration sufficient to inhibit K_{ATP} channel activity in controls, also inhibited channel activity in MIN6-Glib. In contrast, in whole-cell mode, K_{ATP} channel conductance was markedly decreased in MIN6-Glib, suggesting that the number of functional channels at the cell surface is reduced. The pancreatic β -cell K_{ATP} channel comprises Kir6.2 subunits and SUR1 subunits with 4:4 stoichiometry (15–17). Because the SUR1 subunits confer sensitivities to sulfonylureas, we next examined the binding properties and expression of SUR1 in MIN6 cells treated with glibenclamide. Analysis of the glibenclamide binding properties in MIN6 cells

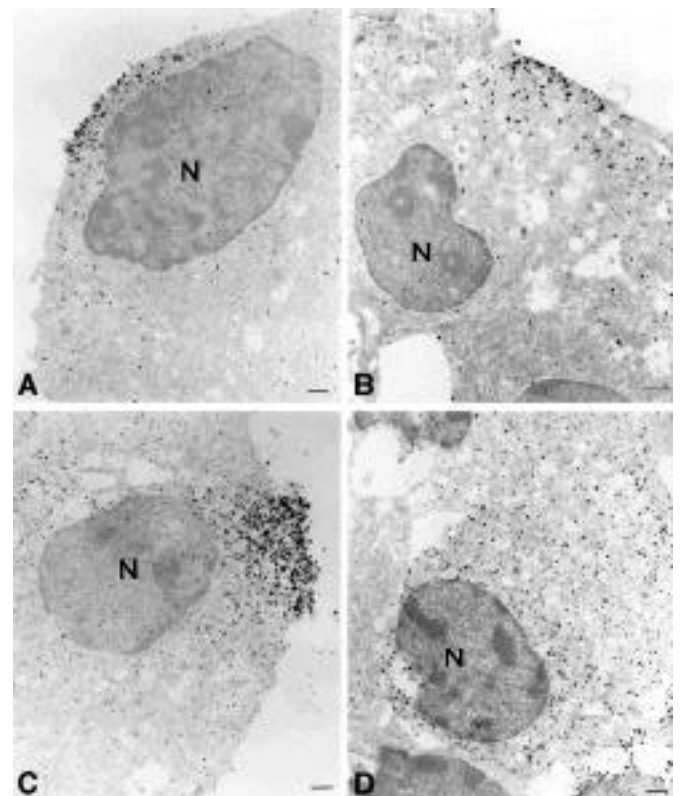


FIG. 7. Electron microscopy showing subcellular localization of SUR1 in control MIN6 cells and MIN6-Glib. The control cell shows a patch-like accumulation of gold particles along the cell membrane (*A, B*), while the particles shift to the deeper regions of the cytoplasm (*C*) or are distributed diffusely in the cytoplasm in MIN6-Glib (*D*). N, nucleus. Bar = 1 μ m.

revealed the presence of high-affinity ($K_{d\text{ high}} = 1.7$ nmol/l) and low-affinity ($K_{d\text{ low}} = 11.6$ nmol/l) binding sites. Interestingly, while chronic glibenclamide treatment did not change the binding affinities of glibenclamide at the two sites, the treatment increased the maximum binding capacities at both sites, as determined by whole-cell binding experiments. In addition, the level of SUR1 protein, as assessed by western blot analysis of whole cells, is increased in MIN6-Glib. Furthermore, electron microscopic examination revealed that a majority of SUR1 are present in a cluster near the cell surface in control MIN6 cells, whereas they are distributed in the deeper region of the cytoplasm or diffusely in the cytoplasm of MIN6-Glib. These results suggest that the reduced K_{ATP} channel activity found in MIN6-Glib is not due to either lack of dissociation of glibenclamide from SUR1 or decreased biosynthesis of SUR1 by glibenclamide, but to a decrease in expression of SUR1 at the cell surface. There are several mechanisms possible for the reduced expression of SUR1 at the cell surface by chronic glibenclamide treatment: it might impair trafficking of SUR1 to the plasma membrane or accelerate internalization of SUR1, and the degradation of SUR1 also might be decelerated. Further studies are necessary to clarify the mechanism.

As described above, we found two glibenclamide binding sites with different affinities in MIN6 cells. It has been reported that the binding affinity of dihydropyridine (DHP) to the $\alpha 1$ subunit is increased in skeletal muscle L-type calcium channels when all the other subunits are coexpressed (31). Accordingly, we thought that the SUR1 subunits might occur

in two conditions in MIN6 cells, some being coupled to Kir6.2 subunits as K_{ATP} channel regulators, while others, not coupled to a Kir6.2 subunit, have an unknown role. Indeed, transfection experiments have confirmed this. While COS-1 cells expressing SUR1 alone or SUR1-Kir6.2 fusion peptide (i.e., SUR1:Kir6.2 = 1:1 stoichiometry) have only one site of low-affinity ($K_{d\text{low}} = 15.5 \text{ nmol/l}$) or high-affinity binding ($K_{d\text{high}} = 5.2 \text{ nmol/l}$), respectively, COS-1 cells expressing SUR1 and Kir6.2 have both the low- and high-affinity binding sites ($K_{d\text{low}} = 15.6 \text{ nmol/l}$, $K_{d\text{high}} = 5.2 \text{ nmol/l}$). The low-affinity site for glibenclamide found in the present study is apparently different from that reported previously in various pancreatic β -cell preparations (32), inasmuch as there is a large difference in the K_d value between the present results and those in previous reports (11.6 nmol/l vs. 0.1–16 $\mu\text{mol/l}$). However, whether or not there is a site of considerably lower affinity for glibenclamide in MIN6 cells is not known.

The present study may have important implications clinically in regard to sulfonylurea treatment in type 2 diabetes. Our data suggest that chronic sulfonylurea treatment could cause a defect in sulfonylurea-induced insulin secretion by reducing the number of functional K_{ATP} channels on the cell surface. Since the sulfonylureas used in clinical practice all have different potencies in receptor binding, inhibition of K_{ATP} channel activity, and insulin secretion (32–34), it is important in future studies to compare the outcomes of chronic treatment among the various sulfonylureas in terms of the clinical implications.

ACKNOWLEDGMENTS

This study was supported by Grant-in-Aid for Creative Basic Research (10NP0201) from the Ministry of Education, Science, Sports and Culture, Japan; by research grants from the Ministry of Health and Welfare, Japan; by a grant for studies on the pathophysiology and complications of diabetes from Tsumura Pharma; by a grant from Novo-Nordisk Pharma; by a grant from Yamanouchi Foundation for Research on Metabolic Disorders; and by a grant from Takeda Chemical Industries.

REFERENCES

- Lebovitz HE: Oral antidiabetic agents. In *Joslin's Diabetes Mellitus*. 13th ed. Kahn CR, Weir GC, Eds. Malvern, PA, Lea & Febiger, 1994, p. 508–529
- Henquin JC: Tolbutamide stimulation and uninhibition of insulin release: studies of the underlying ionic mechanism in isolated rat islet. *Diabetologia* 18:151–160, 1980
- Strugess NC, Ashfold MLJ, Cook DL, Hales CN: The sulfonylurea receptor may be an ATP-sensitive potassium channel. *Lancet* 8453:474–475, 1985
- Trube G, Rorsman P, Ohno-Shosaku T: Opposite effects of tolbutamide and diazoxide on the ATP-dependent K^+ channel in mouse pancreatic β -cells. *Pflugers Arch* 407:493–499, 1986
- Cook DL, Stain LS, Ashfold MLJ, Hales CN: ATP-sensitive K^+ channels in pancreatic β -cells. *Diabetes* 37:495–498, 1988
- Ashcroft FM, Rorsman P: Electrophysiology of the pancreatic β -cell. *Prog Biophys Mol Biol* 54:87–143, 1989
- Henquin JC: Cell biology of insulin secretion. In *Joslin's Diabetes Mellitus*. 13th ed. Kahn CR, Weir GC, Eds. Malvern, PA, Lea & Febiger, 1994, p. 56–80
- Miki T, Nagashima K, Tashiro F, Kotake K, Yoshitomi H, Tamamoto A, Gono T, Iwanaga T, Miyazaki J-I, Seino S: Defective insulin secretion and enhanced insulin action in K_{ATP} channel-deficient mice. *Proc Natl Acad Sci U S A* 95:10402–10406, 1998
- Inagaki N, Tsuura Y, Namba N, Masuda K, Gono T, Horie M, Seino Y, Mizuta M, Seino S: Cloning and functional characterization of a novel ATP-sensitive potassium channel ubiquitously expressed in rat tissues, including pancreatic islets, pituitary, skeletal muscle, and heart. *J Biol Chem* 270:5691–5694
- Inagaki N, Gono T, Clement JP IV, Namba N, Inazawa J, Gonzalez G, Aguilar-Bryan L, Seino S, Bryan J: Reconstitution of IK_{ATP} : an inward rectifier plus the sulfonylurea receptor. *Science* 270:1166–1170, 1995
- Sakura H, Ämmälä C, Smith PA, Gribble FM, Ashcroft FM: Cloning and functional expression of the cDNA encoding a novel ATP-sensitive potassium channel subunit expressed in pancreatic β -cells, brain, heart and skeletal muscle. *FEBS Lett* 377:338–344, 1995
- Aguilar-Bryan L, Nichols CG, Wechsler SW, Clement JP IV, Boyd AE III, Gonzalez G, Herrera-Sosa H, Nguy K, Bryan J, Nelson DA: Cloning of the β -cell high-affinity sulfonylurea receptor: a regulator of insulin secretion. *Science* 268:423–426, 1995
- Inagaki N, Gono T, Clement JP IV, Wang C-Z, Aguilar-Bryan L, Bryan J, Seino S: A family of sulfonylurea receptors determines the pharmacological properties of ATP-sensitive K^+ channels. *Neuron* 16:1011–1017, 1996
- Isomoto S, Kondo C, Yamada M, Matsumoto S, Higashiguchi O, Horio Y, Matsuzawa Y, Kurachi Y: A novel sulfonylurea receptor forms with BIR (Kir6.2) a smooth muscle type ATP-sensitive K^+ channel. *J Biol Chem* 271:24321–24324, 1996
- Inagaki N, Gono T, Seino S: Subunit stoichiometry of the pancreatic β -cell ATP-sensitive K^+ channel. *FEBS Lett* 409:715–720, 1997
- Clement JP IV, Kunjilwar K, Gonzalez G, Schwanstecher M, Panten U, Aguilar-Bryan L, Bryan J: Association and stoichiometry of K_{ATP} channel subunits. *Neuron* 18:827–838, 1997
- Shyng S-L, Nichols CG: Octameric stoichiometry of the K_{ATP} channel complex. *J Gen Physiol* 110:655–664, 1997
- Ashcroft FM, Gribble FM: Correlating structure and function in ATP-sensitive K^+ channels. *Trends Neurosci* 21:288–294, 1998
- Aguilar-Bryan L, Clement JP IV, Gonzalez G, Kunjilwar K, Babenko A, Bryan J: Toward understanding the assembly and structure of K_{ATP} channels. *Physiol Rev* 78:227–245, 1998
- Seino S: ATP-sensitive potassium channels: a model of heteromultimeric potassium channel/receptor assemblies. *Annu Rev Physiol* 61:337–362, 1999
- Karam JH, Sanz E, Salomon E, Nolte MS: Selective unresponsiveness of pancreas B-cells to acute sulfonylurea stimulation during sulfonylurea therapy in NIDDM. *Diabetes* 35:1314–1320, 1986
- Gullo D, Rabuazzo AM, Vetri M, Gatta C, Vinci C, Buscema M, Vigneri R, Purrelo F: Chronic exposure to glibenclamide impairs insulin secretion in isolated rat pancreatic islets. *J Endocrinol Invest* 14:287–291, 1991
- Davalli MA, Pontiroli AE, Socci C, Bertuzzi F, Fattor B, Braghi S, Carlo VD, Pozza G: Human islet chronically exposed in vitro to different stimuli become unresponsive to the same stimuli given acutely: evidence supporting specific desensitization rather than β -cell exhaustion. *Endocrinology* 74:790–794, 1992
- Rabuazzo AM, Buscema M, Vinci C, Caltabiano V, Vetri M, Forte F, Vigneri R, Purrelo F: Glyburide and tolbutamide induce desensitization of insulin release in rat pancreatic islets by different mechanisms. *Endocrinology* 131:1815–1820, 1992
- Gono T, Mizuno N, Inagaki N, Kuromi H, Seino Y, Miyazaki J-I, Seino S: Functional neuronal ionotropic glutamate receptors are expressed in the non-neuronal cell line. *J Biol Chem* 269:16989–16992, 1994
- Tsuura Y, Ishida H, Okamoto Y, Kato S, Sakamoto K, Horie M, Ikeda H, Okada Y, Seino Y: Glucose sensitivity of ATP-sensitive K^+ channel is impaired in β -cells of the GK rat. *Diabetes* 42:1446–1453, 1993
- Ihara Y, Yamada Y, Fujii Y, Gono T, Yano H, Yasuda K, Inagaki N, Seino Y, Seino S: Molecular diversity and functional characterization of voltage-dependent calcium channels (CACN4) expressed in pancreatic β -cells. *Mol Endocrinol* 9:121–130, 1995
- Miki T, Tashiro F, Iwanaga T, Nagashima K, Yoshitomi H, Aihara H, Nitta Y, Gono T, Inagaki N, Miyazaki J-I, Seino S: Abnormalities of pancreatic islets by targeted expression of a dominant-negative K_{ATP} channel. *Proc Natl Acad Sci U S A* 94:11969–11973, 1997
- Ämmälä C, Moorhouse A, Gribble F, Ashfield R, Proks P, Smith PA, Sakura H, Coles B, Ashcroft SJH, Ashcroft FM: Promiscuous coupling between the sulfonylurea receptor and inwardly rectifying potassium channels. *Nature* 379:545–548, 1996
- Sambrook J, Fritsch EF, Maniatis T: *Molecular Cloning: A Laboratory Manual*. 2nd ed. Ford N, Nalon C, Ferguson M, Eds. Cold Spring Harbor, NY, Cold Spring Harbor Laboratory Press, 1989, p. 7.1–7.87
- Suh-Kim H, Wei X, Birnbaumer L: Subunit composition is a major determinant in high affinity binding of a Ca^{2+} channel blocker. *Mol Pharmacol* 50:1330–1337, 1996
- Ashcroft SJH, Ashcroft FM: The sulfonylurea receptor. *Biochim Biophys Acta* 1175:45–59, 1992
- Schmid-Antomarchi H, Weille JD, Fosset M, Lazdunski M: The receptor for antidiabetic sulfonylureas controls the activity of the ATP-modulated K^+ channel in insulin-secreting cells. *J Biol Chem* 262:15840–15844, 1987
- Gribble FM, Tucker SJ, Seino S, Ashcroft FM: Tissue specificity of sulfonylurea: studies on cloned cardiac and β -cell K_{ATP} channels. *Diabetes* 47:1412–1418, 1998